Performance analysis of a new deep super-cooling two-stage organic Rankine cycle

Y. Yuan[a], G. Xu[a], Y. Quan[a,*], H. Wu[b,**], G. Song[a], W. Gong[a], X. Luo[a]

[a]National Key Lab. of Science and Technology on Aero-thermodynamics, School of Energy and Power Engineering, Beihang University, Beijing 100191, China.

[b]School of Engineering and Technology, University of Hertfordshire, Hatfield, AL10 9AB, United Kingdom

[*]Corresponding author. Email: quanyongkai@buaa.edu.cn Tel. +86(010)82338335
[**]Corresponding author. Email: h.wu6@herts.ac.uk Tel. +44(0)1707 284265, Fax.:+44(0)1707 285086

Abstract

In this article, a new deep super-cooling two-stage organic Rankine cycle (DTORC) is proposed and evaluated at high temperature waste heat recovery in order to increase the power output. A thermodynamic model of recuperative organic rankine cycle (ORC) is also established for the purpose of comparison. Furthermore, a new evaluation index, effective heat source utilization, is proposed to reflect the relationship among the heat source, power output and consumption of the waste heat carrier. A simulation model is formulated and analysed under a wide range of operating conditions with the heat resource temperature fixed at 300 ℃. Hexamethyldisiloxane (MM) and R245fa are used as the working fluid for DTORC, and MM for ORC. In the current work, the comparisons of heat source utilization, net thermal efficiency as well as the total surface area of the heat exchangers between DTORC and RC are discussed in detail. Results show that the DTORC performs better than ORC at high temperature waste heat recovery and it could increase the power output by 150%. Moreover, the maximum net thermal efficiency of DTORC can reach to 23.5% and increased by 30.5% compared with that using ORC, whereas the total surface areas of the heat exchangers are nearly the same.

Keywords: High temperature waste heat; deep super-cooling; two-stage; organic Rankine cycle; effective heat source utilization.

Nomenclature

h	specific enthalpy, kJ/kg
$\dot{m}$	mass flow rate, kg/s
P	pressure, kPa
Q	quantity of heat, kJ
t/T	temperature,℃
W	power, kW
Sur_{total}	the total surface area of heat exchangers, m^2
η_{net}	net thermal efficiency, %
$\eta_{utilization}$	heat source utilization, %

Greek letters

η	efficiency, %

Subscripts

ab	absorb
c	critical state
dis	discharge
exp	expander
HTF	heat transfer fluid
$HTFin$	the heat transfer fluid inlet the evaporator
$HTFout$	the heat transfer fluid outlet the evaporator
loss	loss
max1	the maximum of first stage
max2	the maximum of second stage
min1	the minimum of first stage
net	net
p	pump
pinch	pinch point temperature difference
rec	recuperate
s	isentropic state
sys	the whole system
set	user settings
sur	surrounding
subcool	subcooled status
MM	the MM system
R245fa	the R245fa system
1-23	points on plant scheme or in *T-s* diagram

Abbreviations

BORC	basic organic Rankine cycle
CHP	combined heat and power
DTORC	deep super-cooling two-stage organic Rankine cycle
EHE	external heat exchanger
HTF	heat transfer fluid
ICE	internal combustion engine
IHE	inner heat exchanger
MM	hexamethyldisiloxane
MDM	octamethyltrisiloxane
ORC	organic Rankine cycle
RC	recuperative ORC
R245fa	perfluoropropane
TORC	two-stage ORC
WHC	waste heat carrier

1. Introduction

With rapidly increasing globalization and energy demands, researchers are devoted to seeking opportunities to improve the energy efficiency. Among the energy-efficient technologies, organic Rankine cycle (ORC) is considered as one of the most attractive ways to solve the energy crisis in the future [1]. Over the past two decades, a number of research efforts have been devoted to the studies of ORC on solar thermal [2, 3], geothermal [4, 5], internal combustion engine(ICE) [6, 7], combustion gas turbine [8, 9], combined heat and power (CHP) [10], waste heat from power plants [11] and industrial processes [12, 13]. For those above application, it is recognized that the heat source temperature is usually in the range of 250-350 °C. Gao et al. [3] developed an ORC system driven by solar energy and the high temperature of the system can be up to 300 °C. Sarkar [14] pointed out that the waste heat at temperatures can be 300-400 °C in some industries such as iron and steel, glass, nonferrous metals, bricks and ceramics processing. Peris et al. [12] summarized the wide range of the waste heat source temperatures from industrial gases and over 60% were in the temperature range of 250-350 °C.

For the case of high temperature waste heat recovery applications, thermal systems should have a high thermal stability requirement against the working fluid. Nowadays, most of the ORC manufacturers [15] and researchers [3, 16] are using siloxanes as the working fluids as they have the desired characteristics in reaching high working temperatures and are more thermally stable and environmentally friendly. However, siloxanes are dry organic fluids [17] and have a large sensible heat in isobaric heat discharging sub-process, therefore, recuperative ORC is used in the existing systems. It can significantly improve the thermal efficiency of the system, however, it is difficult to improve the utilization level of the high temperature waste heat sources.

In the ORC system, the inner heat exchanger (IHE) leads to a high exhaust temperature of the waste heat carrier (WHC) [18, 19]. The WHC can be a fluid, steam or exhaust gases and often forms an open loop. The IHE only shifts part of the sensible heat in the isobaric heat discharging sub-process from the working fluid to the WHC. This sensible heat will not be converted into power rather will be discharged to the environment carried by the WHC. For a certain waste heat source, ORC system may consume much more waste heat carrier than a basic

ORC (BORC) system under the same power output since the BORC can absorb more heat from the unit mass flow rate of the waste heat carrier. In such situations, the extra consumption of the mass flow rate of the waste heat carrier can lead to the resource wastage.

Compared with IHE, the external heat exchanger (EHE) can also take advantage of the heat in the isobaric heat discharging sub-process. EHE can transfer such heat to an extra ORC acting as an evaporator. This system is called two-stage organic Rankine cycle (TORC). Kosmadakis et al. [20] introduced a TORC for reverse osmosis (RO) desalination. In their work the condenser of the high temperature stage acted as the evaporator of the low temperature stage. They used R245fa at high temperature stage and HFC-134a at low temperature stage. Xue et al. [21] proposed a TORC using R227ea and R116 as the working fluids at high and low temperature stage, respectively. Thierry et al. [22] studied the mixtures as the working fluid in TORC, and improved the amount of energy recovery. All these TORC mentioned above are used at low temperature waste heat recovery and have not been applied at high temperature.

Furthermore, how to evaluate the utilization of the heat source and the performance of the thermal systems is also an important issue. Over the past decades, evaluation indexes are mainly concentrated on the economic cost, thermal efficiency and exergy efficiency [23-27]. Some researchers also take the maximum power output as the optimization goal [28, 29]. However, few research works take the WHC consumption into account for the performance evaluation. In particular, no evaluation index is available to reflect the relationship among the heat source, power output and WHC consumption. As such, the objective of the current study is to develop a deep super-cooling two-stage organic Rankine cycle (DTORC) based on the traditional TORC with fully utilize the high temperature waste heat and increase the power output. In addition, a new evaluation index, effective heat source utilization, is also defined which will evaluate the

ORC systems. The detailed description of DTORC is given in section 2. The new evaluation index is explained and the thermodynamic models of DTORC and RC are established in section 3. Finally, the DTORC and RC systems are compared under the same heat source and discussed in section 4. The three key performance indicators: heat source utilization, net thermal efficiency and total surface area of heat exchangers are compared in a systematic manner.

2. System description of DTORC

In the current study, a DTORC system has been developed, as shown in Fig. 1. First, the waste heat is transformed to mechanical energy through the high temperature organic Rankine cycle, this can be regarded as the “high temperature stage”. During condensation, the condenser of this high temperature stage will act as the evaporator of the low temperature organic Rankine cycle which is considered as the “low temperature stage”.

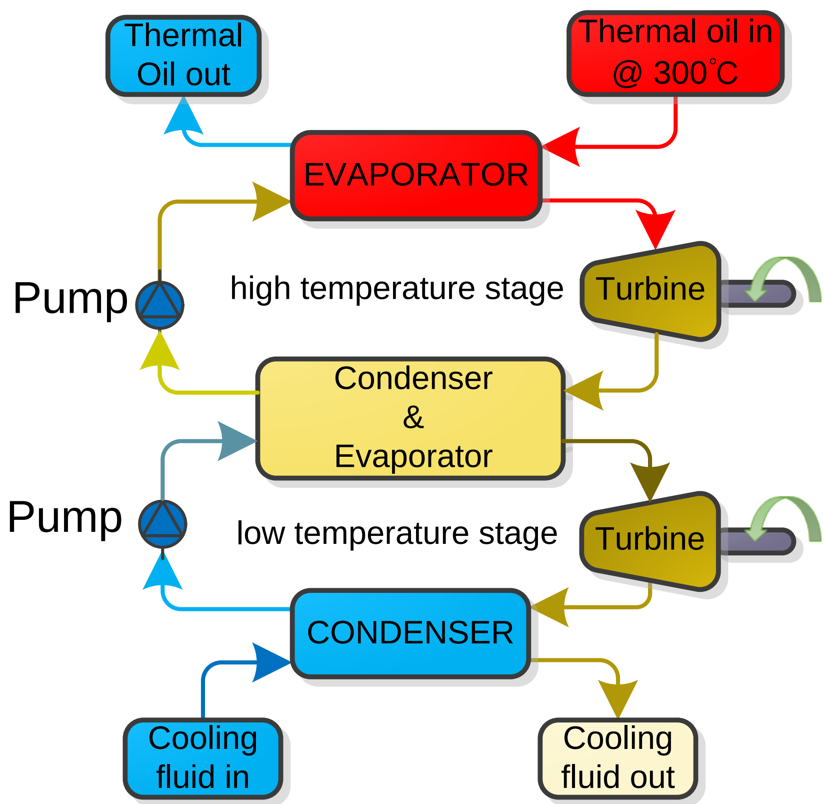

Fig. 1. Schematic diagram of DTORC system.

As the DTORC is used for high temperature waste heat recovery, hexamethyldisiloxane (MM) has been selected for the high temperature stage due to its appropriate thermodynamic properties and optimum thermal stability. The normal boiling point of MM is 100.25 °C. This means the outlet temperature of the high temperature stage turbine can reach 203 °C or higher if the condensation pressure remains positive, as shown in Fig. 2. According to the research of [30], it shows that R245fa is more suitable as the working fluid under such a temperature compared to other working fluids, thus, the refrigerant R245fa has been selected for the low temperature stage. Table 1 lists the characteristics of the working fluids for the DTORC.

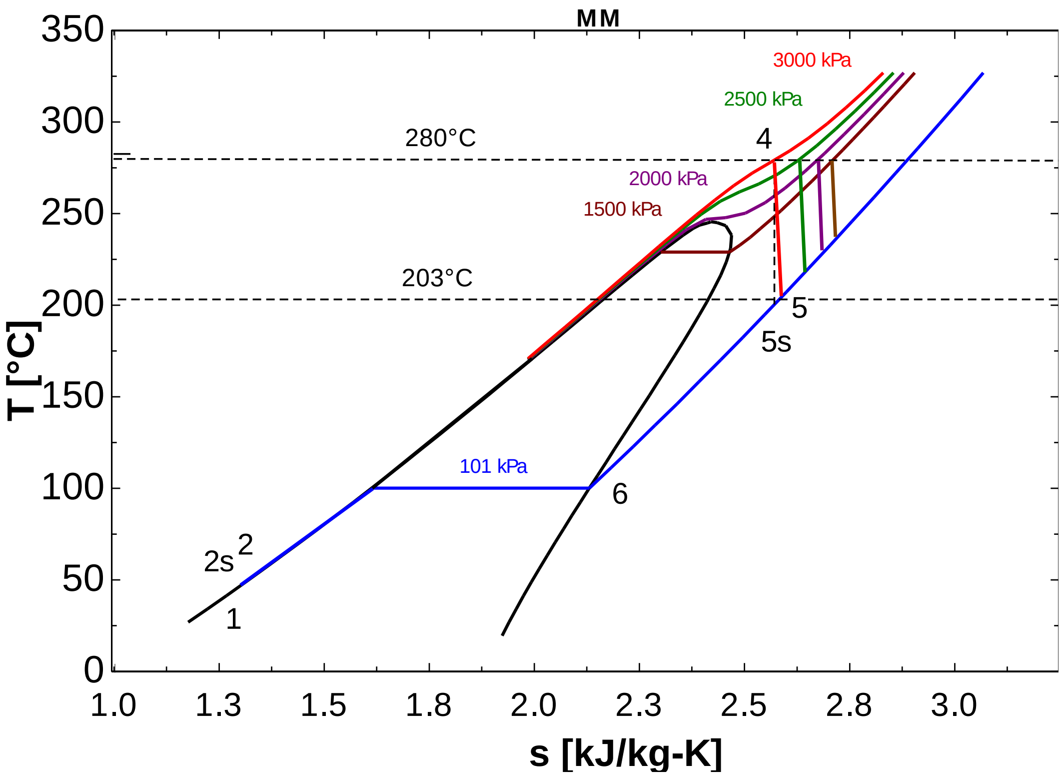

Fig. 2. *T*-*s* diagram of MM.

Table 1

Characteristics and properties of MM and R245fa.

fluid	M (g/mol)	T_{NBP} (℃)	T_C (℃)	P_C (kPa)	ODP	GWP (100 years)	Type	Price ($/10kg)
MM	162,378	100.25	245.55	1939.4	0	0	Dry	61
R245fa	134,045	15.14	154.01	3651.0	0	1030	Dry	251

NBP: Normal boiling point; C: Critical.

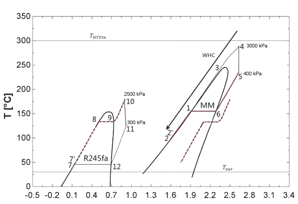

Fig. 3. *T-s* diagram of MM and R245fa.

In the present work, a new deep super-cooling technology was proposed, as shown in Fig. 3. The sub-process (1-2) is the deep super-cooling technology. The processes in DTORC are described as follows:

2′-3-4: The working fluid MM absorbs the heat from the WHC at high temperature stage.

4-5: The supercritical steam of MM enters the turbine to produce power.

5-6-1-2: MM discharges the heat to the low temperature stage. In the traditional TORC cycle, MM discharges heat and ends at point 1. For the current cycle, the low temperature stage makes MM run till the deep super-cooling status and ends at point 2.

2-2′: The deep super-cooling MM is pumped to a high pressure by the feed pump.

7′-8-9-10: The working fluid R245fa of the low temperature stage absorbs the heat from the high temperature stage.

10-11: The overheating steam of R245fa enters the turbine to produce power.

11-12-7: R245fa discharges the heat to the environment.

7-7′: The liquid R245fa is pumped to a high pressure by the feed pump.

Through the deep super-cooling process (1-2), MM achieves a lower temperature before interring the evaporator. This makes the unit mass of WHC discharge more heat and improves the utilization of the high temperature waste heat. With the aid of this low temperature stage the whole system achieves an additional power output and the overall efficiency increases significantly.

3. System Modeling

In the current work, numerical models of the DTORC (see Fig. 1) and RC (see Fig. 4) systems have been developed using Engineering Equation Solver (EES) which provides an inner fluid property database including those of MM and R245fa. The RC system is selected for the purpose of comparison.

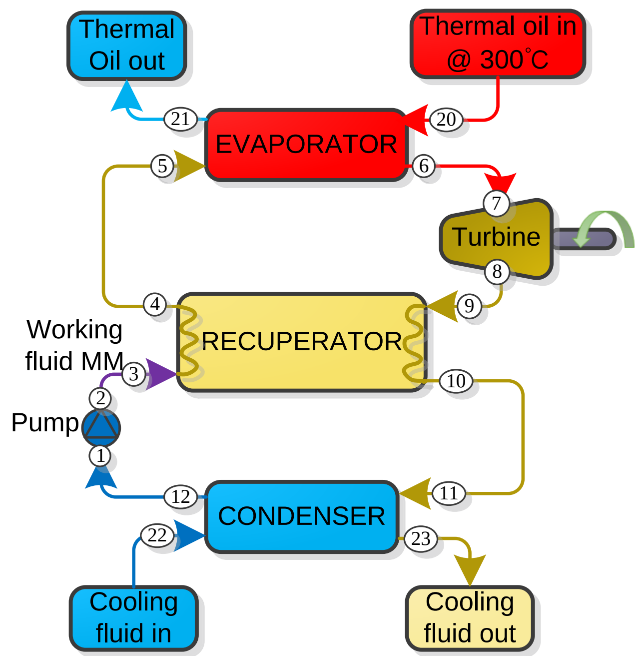

Fig. 4. Schematic diagram of RC system.

3.1. Assumptions and index defined

Thermal oil (THERMINOL® 66, Solutia Inc.) is selected to imitate the WHC. The thermal oil is also called heat transfer fluid (HTF). Some thermodynamic properties of the thermal oil, such as density and enthalpy, are available at temperatures ranging from -7 °C to 371 °C as stated by Solutia Inc. In addition, some assumptions are made as follows:

i. The waste heat carrier has a highest inlet temperature (T_{HTFin}) of 300 °C, and the surrounding temperature (T_{sur}) is assumed to be 30 °C.

ii. The pressure drop is fixed at 20 kPa both in the evaporator and condenser which can be ignored in the pipe. The minimum pressure of DTORC and RC remains positive to prevent air infiltration.

iii. The heat transfer coefficients of the DTORC and RC systems are fixed at 3500 W/m^{2}K by reference to an ordinary plate heat exchanger. It means the total heat transfer area is proportional to the total amount of heat transfer.

iv. The isentropic efficiencies of the pump and expander (η_{exp}&η_p) are considered as constant of 80% and the expansion and compression processes have been assumed to be adiabatic.

$$\eta_p = (h_{2s} - h_1) / (h_2 - h_1) \tag{1}$$

where h_1 and h_2 are the specific enthalpies at the inlet and outlet of the pump respectively (see Fig. 2), and h_{2s} is the specific enthalpy following an isentropic pumping process that starts from the same state at the pump inlet and ends at the same pressure at the pump outlet.

$$\eta_{exp} = (h_4 - h_5) / (h_4 - h_{5s}) \tag{2}$$

where h_{5s} is the specific enthalpy at the expander exit for an isentropic process (see Fig. 2).

v. The pinch temperatures (t_{pinch}) in DTORC and RC are more than 18 °C and all the working fluids remain a superheat of 2 °C to flow into the expander or at least 20 kPa lower than the saturation pressure under the expander inlet temperature.

vi. All systems are modeled under steady state conditions based on the first principle of energy conservation. The entire net power outputs of both DTORC and RC systems are fixed at 200 kW.

Besides, the heat source utilization ($\eta_{utilization}$) is defined as the ratio of the net power output to the total thermal energy of the heat source in which T_{HTFin} and T_{sur} are considered as the reference temperatures:

$$\eta_{utilization} = W_{net} / ((h_{HTF,T_{HTFin}} - h_{HTF,T_{sur}}) * \dot{m}_{HTF}) \tag{3}$$

here $h_{HTF,T_{HTFin}}$ and $h_{HTF,T_{sur}}$ are the specific enthalpies of the waste heat carrier at the temperature of T_{HTFin} and T_{sur} respectively (see Fig. 3), and $\dot{m}_{HTF}$ is the mass flow rate of the WHC. W_{net} is the net power output of the thermal system.

3.2. DTORC system modeling

It is noted that if the deep super-cooling process (1-2) of MM (see Fig. 3) is abandoned and the WHC (thermal oil) leaving the high temperature stage is used to preheat R245fa directly as shown in Fig. 5, the result of the emulational modeling would be divergent. As a result, the current work mainly focuses on the system demonstrated in both Fig. 1 and Fig. 3. For the described cycle, the simulation is performed using an EES-based program. The enthalpy of the THERMINOL® 66 is programmed to be an inner function of EES based on the data provided by manufacturer.

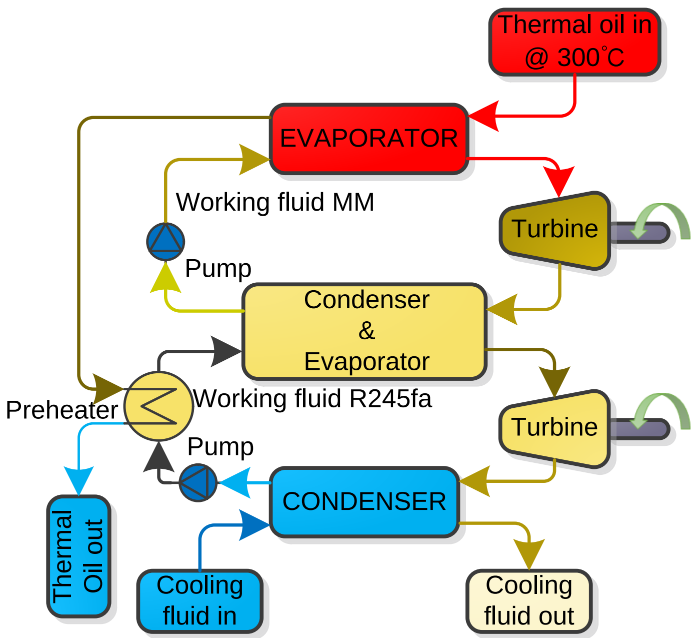

Fig. 5. Schematic diagram of TORC with preheating.

3.2.1. Two notes in the program

In this section, two key factors should be stressed here:

Note 1: as shown in Fig. 3, the process (11-12) in the low temperature stage can also satisfy the inner heat transfer condition which is similar to Fig. 6(b), and the proposed modelling has been designed to determine whether to use a recuperator or not at low temperature stage according to the temperatures at point 14 and point 10 (see Fig. 6a). If the temperature of point

14 is one t_{pinch} higher than that of point 10, then the model will be changed from Fig.6 (a) to Fig. 6(b). As a matter of fact, the use of a recuperator should be avoided at low temperature stage, since it will increase the pump inlet temperature at high temperature stage thus leading to a rise of the evaporator inlet temperature. This will increase the emission temperature of the waste heat carrier and may cause a decline of the heat source utilization. Therefore, isentropic or wet working fluid is suggested for the low temperature stage. Although R245fa is a dry working fluid, its saturated vapor line is very close to that of an isentropic fluid and its temperature profile is suitable for working with MM.

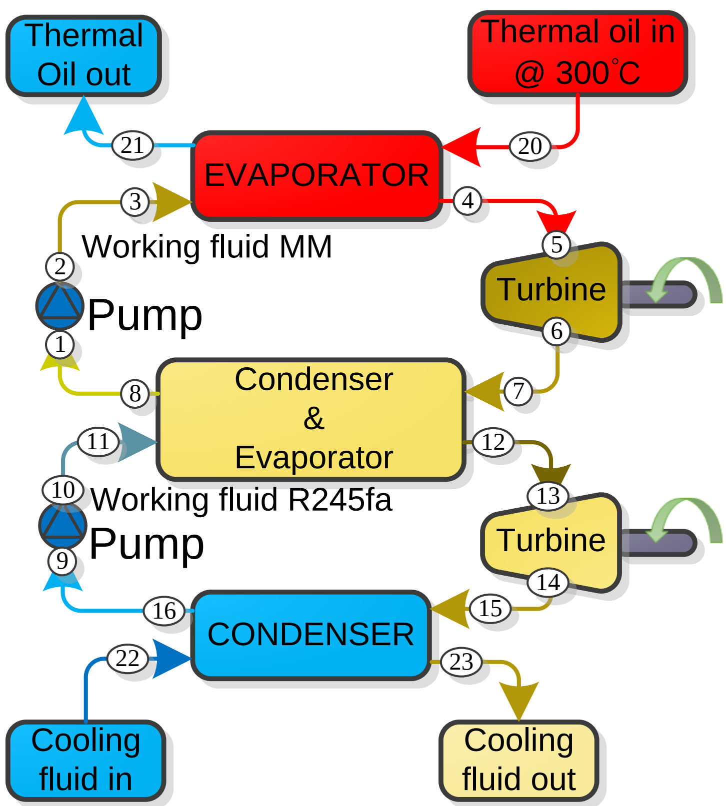

(a)

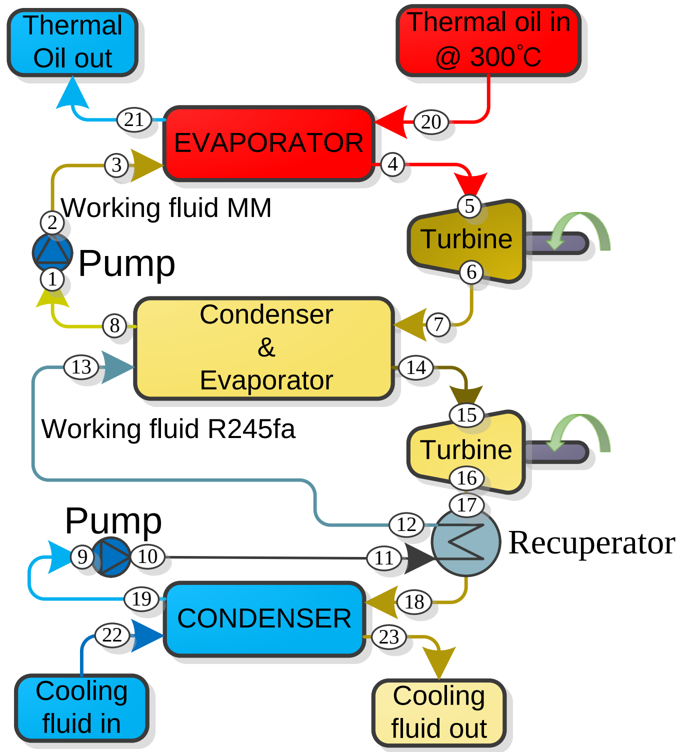

(b)

Fig. 6. Schematic diagram of DTORC system at low temperature stage:

(a) without recuperator; (b) with recuperator.

Note 2: the temperature difference of heat exchange between the process (7-8) and (11-12) (see Fig. 6(a)) should always satisfy t_{pinch} . For example, as shown in Fig. 7, the temperatures at point 7 and 8 are higher than that at point 12 and 11, respectively, but the vaporization temperature of the R245fa cycle is higher than the liquefaction temperature of the MM cycle. This may result in an impractical heat transfer in the thermodynamic model and it should be avoided. In the current study, this can be solved by adding a constraint between the condensation pressure of the MM cycle and the evaporation pressure of the R245fa cycle, and making sure that the evaporating temperature of R245fa is at least one t_{pinch} lower than the condensing temperature of MM.

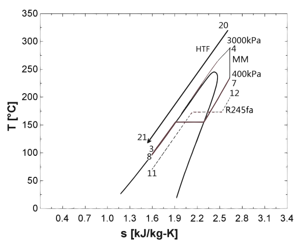

Fig. 7. An impractical heat transfer process between two stages in DTORC.

3.2.2. Flowchart of TORC

The simplified block diagram in Fig. 8 illustrates the basic concept of the DTORC System modeling. In the current modeling, $P_{set,max1}$, $P_{set,min1}$, $P_{set,max2}$, $P_{set,min2}$ and $t_{set,subcool,1}$ are the input parameters. Normally, P_{max1} (pressure after pump in the high temperature stage), P_{min1} (pressure before pump in the high temperature stage), P_{max2} (pressure after pump in the low temperature stage), P_{min2} (pressure after pump in the low temperature stage), and $t_{subcool,1}$ (super-cooling degree of MM in the high temperature stage) are equal to the input parameters. However, in some cases, the input parameters are in conflict with the boundary conditions, then the "**Protection program**" will limit P_{max1}, P_{min1}, P_{max2}, P_{min2}, and $t_{subcool,1}$ in a reasonable range. Meanwhile, P_{max1}, P_{min1}, P_{max2}, P_{min2} and $t_{subcool,1}$, which are determined by the anticipant input parameters and boundary conditions, are presented in an clear manner.

As shown in Fig. 3:

$$t_{subcool,1} = T_1 - T_2 \tag{4}$$

There is a maximum $t_{subcool,1}$ to make T_2 one t_{pinch} higher than $T_{7'}$, which is the pump outlet temperature of the R245fa cycle. When the anticipant $t_{set,subcool,1}$ exceeds the maximum $t_{subcool,1}$, the "**Protection program**" will use the maximum $t_{subcool,1}$; $P_{set,max1}$ is the anticipant pump outlet pressure of MM ($P_{2'}$); If the "**Protection program**" detects that the state of MM at point 4 does not satisfy assumption(v), the program will limit P_4 to the maximum pressure under T_4 and change the value of P_{max1}; P_{min1} (P_2) and P_{min2} (P_7) should be positive to prevent air infiltration; P_{max2} ($P_{7'}$) should satisfy both assumption(v) and Note 2.

Note 1 will be achieved automatically by the "**Judgment program**", and a new calculation module - **Main calculation module 2** will be used.

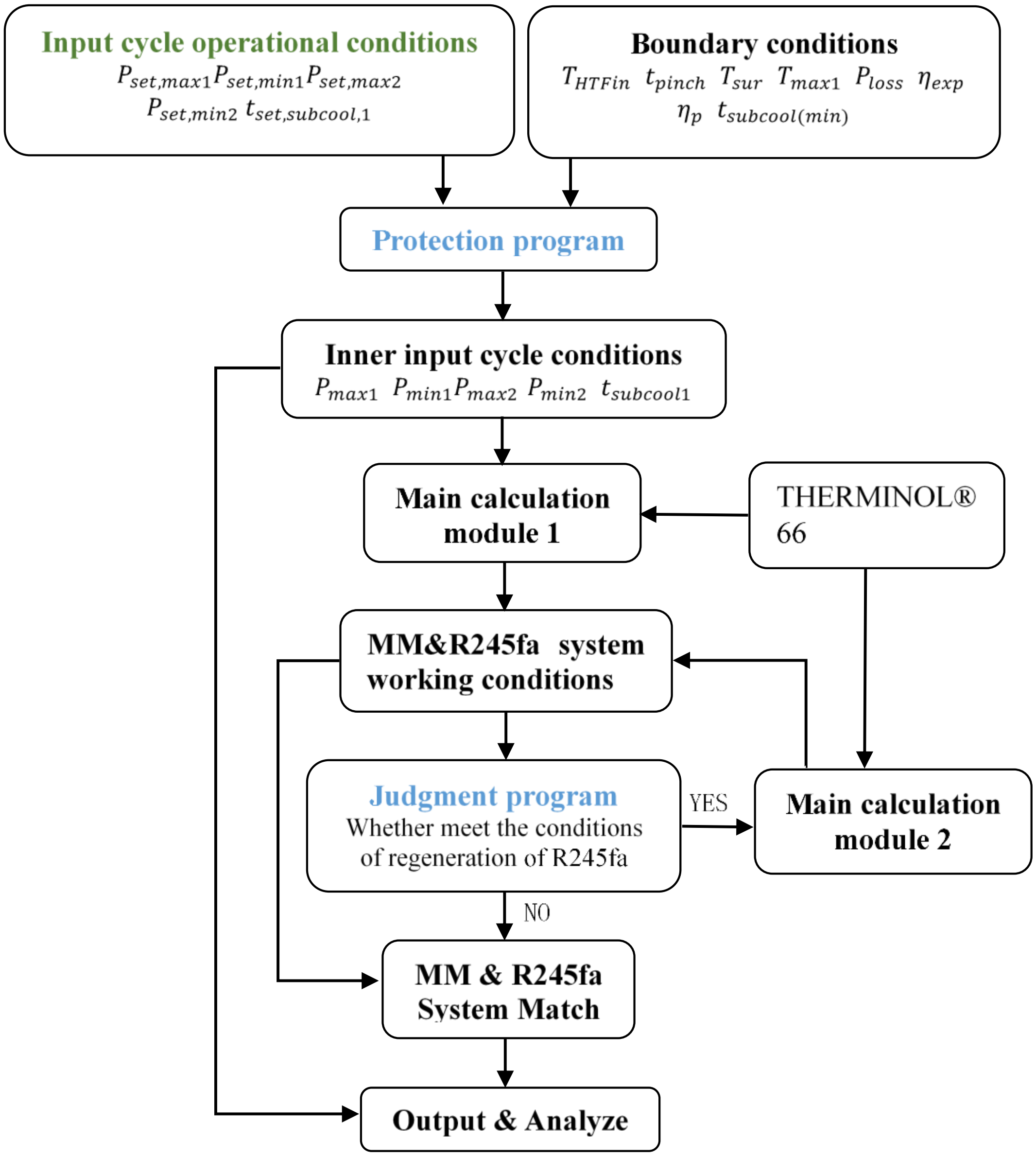

Fig. 8. Flowchart of DTORC system.

3.2.3. Formulas of DTORC

The main formulas used in the simulation are based on enthalpy and entropy changes. Pressure and temperature codetermine the enthalpy of a specific point except in the vaporization process and liquefaction process. There is a one-to-one correspondence between saturation temperature and saturation pressure. The enthalpy of the HTF is correlated with temperature in terms of the specification supported by the manufacturer. More details can be obtained from the Appendix.

3.3. RC system modeling

It is mentioned above that T_{HTFin} is around 300 °C, and MM is also selected as the working fluid for the RC system. Considering the large positive inclination of the vapor saturation line of MM as demonstrated in Fig. 2, a recuperator is used to improve the thermal efficiency. The schematic drawing of the RC system using MM is presented in Fig. 4. The main program flowchart of the RC system is illustrated in Fig. 9. For the purpose of comparison, the RC system runs under the same heat source as the DTORC system. The main formula of the RC system is similar to that of the low temperature stage of the DTORC system in Fig. 6(b).

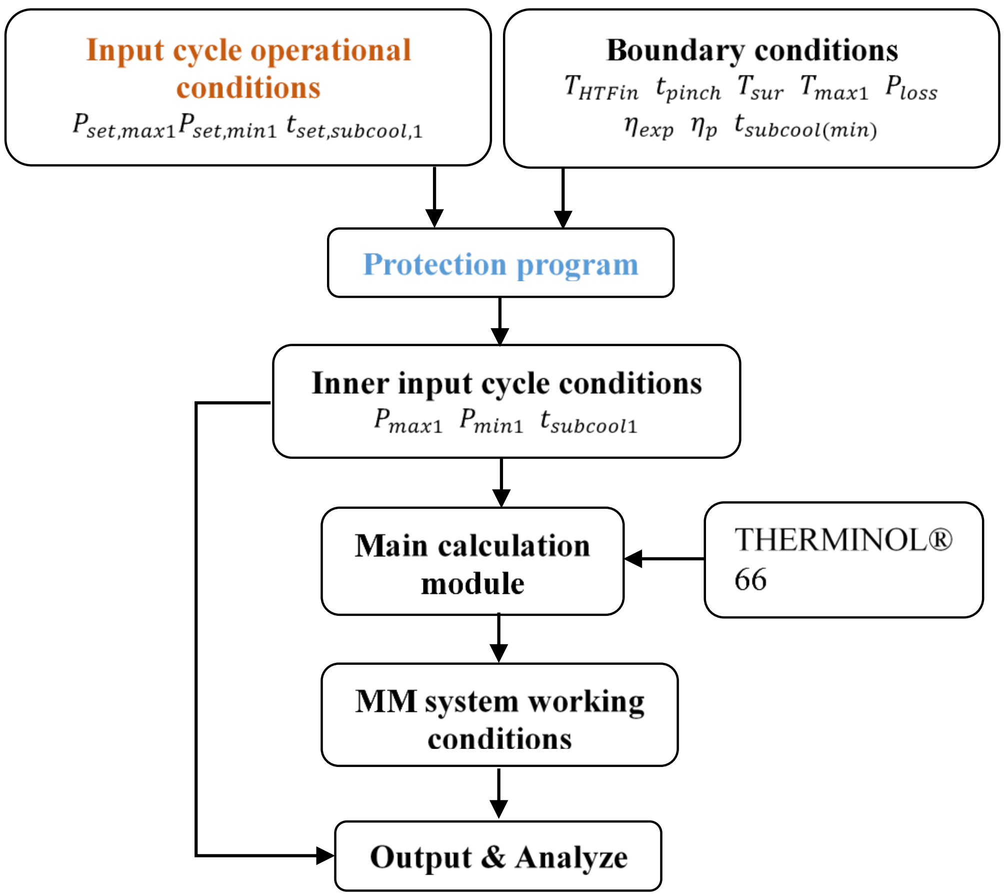

Fig. 9. Flowchart of RC system.

4. Results and discussion

In the current study, the overall net power output is fixed at 200 kW and the temperature of the heat source is 300 °C. By comparing η_{net}, $\eta_{utilization}$ and Sur_{total}, the performance analysis of DTORC is achieved. In order to analyze the effect of the working fluids on the DTORC system, different power outputs at two stages are shown in the following sections.

4.1. Thermal efficiency and heat source utilization

Unlike exergy efficiency, the heat source utilization mainly focuses on the entropy generation caused by the temperature difference. When the WHC is discharged into the environment at a high residual temperature which is not completely utilized, the thermal efficiency and exergy efficiency may still be quite high but $\eta_{utilization}$ is low. It will take the whole heat source into account and higher $\eta_{utilization}$ means lower WHC consumption under the same power output.

In the DTORC system, P_{max2} and P_{min2} are set to be maximum and minimum respectively which can make the low temperature stage achieve maximum thermal efficiency at a certain heat source. The heat source of the low temperature stage is determined by P_{min1} of the high temperature stage. The condensation temperature of the low temperature stage is determined by T_{sur}. P_{max1}, P_{min1} and $t_{subcool1}$ are changed to get the general rule of η_{net} and $\eta_{utilization}$ of the DTORC.

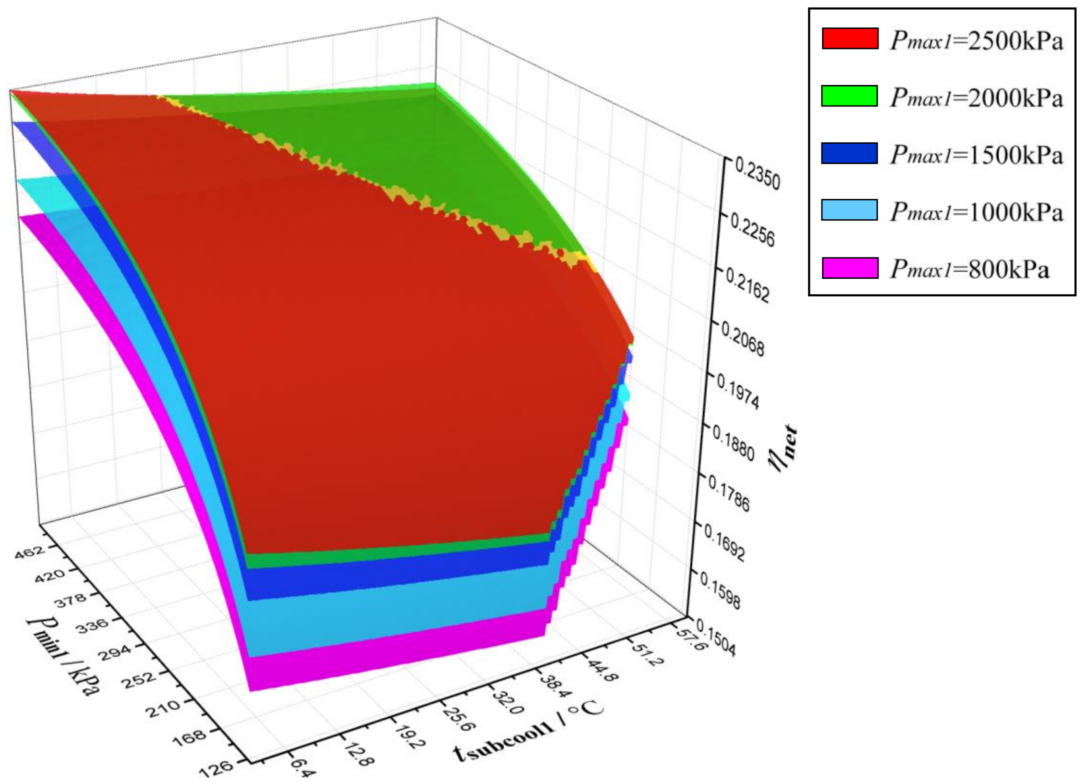

Fig. 10. Net thermal efficiency of DTORC under different P_{max1}.

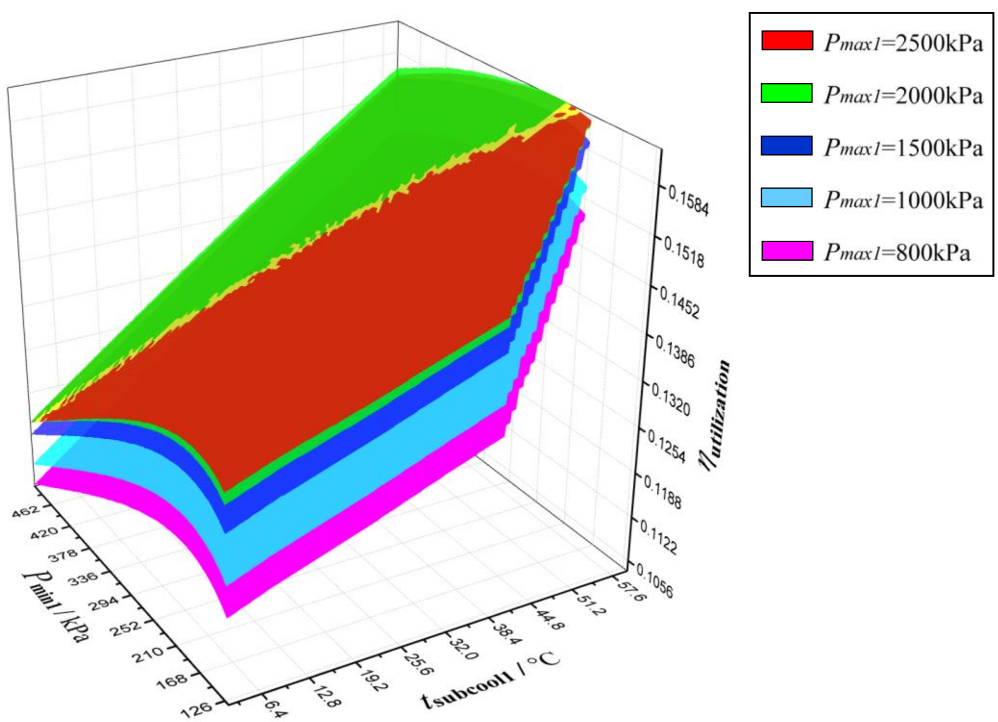

Fig. 11. Heat source utilization of DTORC under different P_{max1}.

Fig. 10 and Fig. 11 show the influences of P_{min1} and $t_{subcool1}$ on η_{net} and $\eta_{utilization}$ under different P_{max1}. It is found that both η_{net} and $\eta_{utilization}$ increase with the increase of P_{max1}, but when P_{max1} exceeds 2000 kPa, η_{net} and $\eta_{utilization}$ decrease in some areas. When P_{max1} is lower than P_c (1939.4 kPa), the addition of P_{max1} can increase the mean evaporation temperature of the high temperature stage which leads to a gain of η_{net}. When P_{max1} exceeds P_c, the increase of P_{max1} has a weak effect on η_{net}, and the pump power consumption becomes more and more visible. The higher the P_{max1}, the more pump power it consumes. The increase of η_{net} caused by the increased P_{max1} will be offset by the reduction of η_{net} caused by the pump and thus lead to a reduced η_{net} in some areas, as shown Fig.10. The reduction of $t_{subcool1}$ leads to an increase of η_{net}. This can be explained by the fact that the heat of the subcooled process (1-2) (see Fig. 3) conducts itself to the low temperature stage. As there is pinch point temperature difference in heat transfer, this means a quality reduction of the thermal energy for the low temperature stage, and this will certainly result in a reduction of η_{net}. It is clear that the higher $t_{subcool,1}$ is the lower η_{net} would be. But this can in some way increase $\eta_{utilization}$ as it reduces T_{HTFout} and the mass flow rate of WHC. Meanwhile, the rise of P_{min1} increases the mean evaporation temperature of the low temperature stage which will lead to an increased η_{net}, and it also increases the mean condensation temperature at high temperature stage which will lead to a reduced η_{net}. But the second stage contributes much more to η_{net} than the first stage, and the comprehensive result is an increase of η_{net}. Although the increase of $t_{subcool,1}$ reduces η_{net} and leads to an increase of Q_{absorb}, it will also lead to a reduction of heat source consumption thus resulting in an increase of $\eta_{utilization}$, as shown in Fig.11. With $\eta_{utilization}$ up to its maximum value of 16.3%, DTORC could obtain a η_{net} of 20.2% when P_{max1} is about 2000 kPa, P_{min1} 239 kPa and $t_{subcool1}$ 60 °C. Meanwhile, the highest temperature of the low temperature stage is 228℃. The maximum η_{net} of DTORC reaches up to 23.5%.

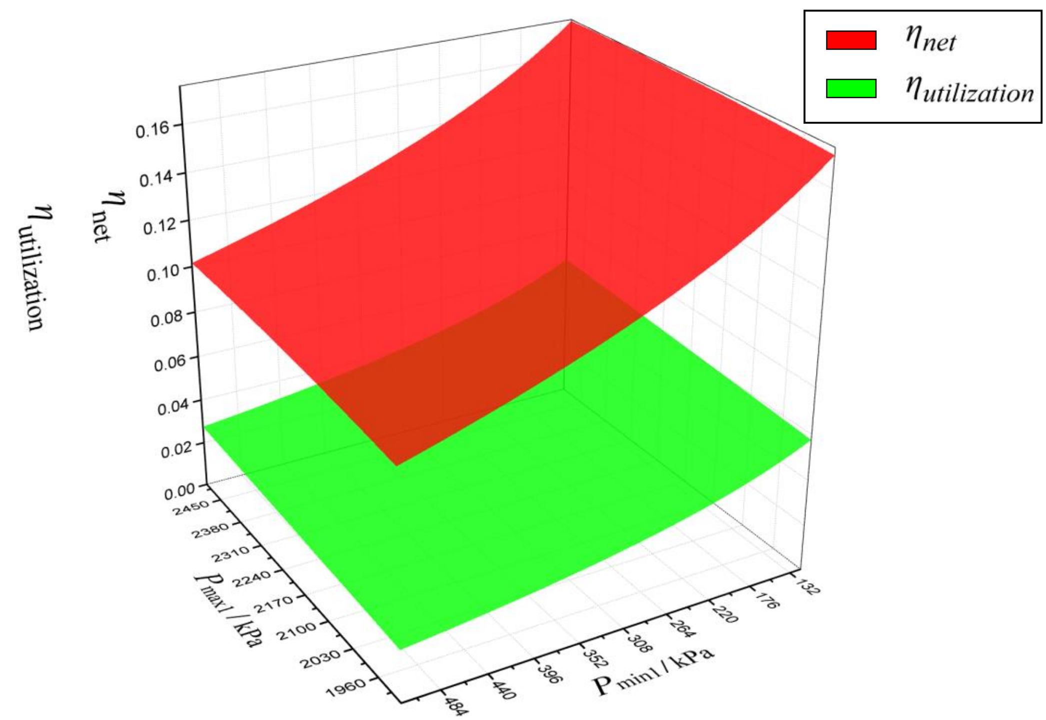

Fig. 12. Net thermal efficiency and heat source utilization of RC.

Fig. 12 shows $\eta_{utilization}$ and η_{net} of the RC system. Unlike the DTORC system, $\eta_{utilization}$ and η_{net} of the RC system decline with the increasing of P_{min1}. It shows that $\eta_{utilization}$ and η_{net} have the same trend, but η_{net} is more sensitive to P_{min1} than $\eta_{utilization}$. For a certain power output in this RC system, the higher η_{net} is the less $\dot{m}_{HTF}$ would be consumed. And this will result in a high $\eta_{utilization}$. The drop of P_{min1} reduces the mean condensation temperature, leading to the increase of η_{net}. The drop of P_{min1} also reduces the outlet temperature of the expander which will cause a decline of inlet temperature of the evaporator. These lead to a reduction of $\dot{m}_{HTF}$ and will improve $\eta_{utilization}$ (see Eq. 3). As P_{max1} has already exceeded the P_C, as shown in Fig. 12, the increase of P_{max1} will barely contribute to η_{net}. The maximum $\eta_{utilization}$ and η_{net} of RC are up to 6.5% and 18%, respectively.

As a consequence, under the same heat source and positive condensation pressure, the η_{net} of DTORC has a maximum increase of 30.5% greater than RC's. And $\eta_{utilization}$ of the DTORC system is almost two and a half times of RC system. In other words, the use of DTORC could increase the power output by 150% under the same mass flow rate of WHC.

4.2. Total surface area of heat exchangers (Sur_{total})

For a certain heat exchanger, the area needed is related to the mean temperature difference, surface heat transfer coefficient and total amount of heat transfer. Based on assumption (iii), the temperature difference is assumed to be t_{pinch} and the heat transfer coefficient is 3500 W/m^{2}K. In the DTORC, Sur_{total} equals the evaporator and condenser surface areas of the MM cycle plus the condenser and recuperator (if any) surface areas of the R245fa cycle. The condenser of the MM cycle is also the evaporator of the R245fa cycle. The influence of P_{min1} and $t_{subcool,1}$ on the Sur_{total} of DTORC at different P_{max1} is shown in Fig. 13. The influence of P_{min1} and P_{max1} on the Sur_{total} of RC is shown in Fig. 14.

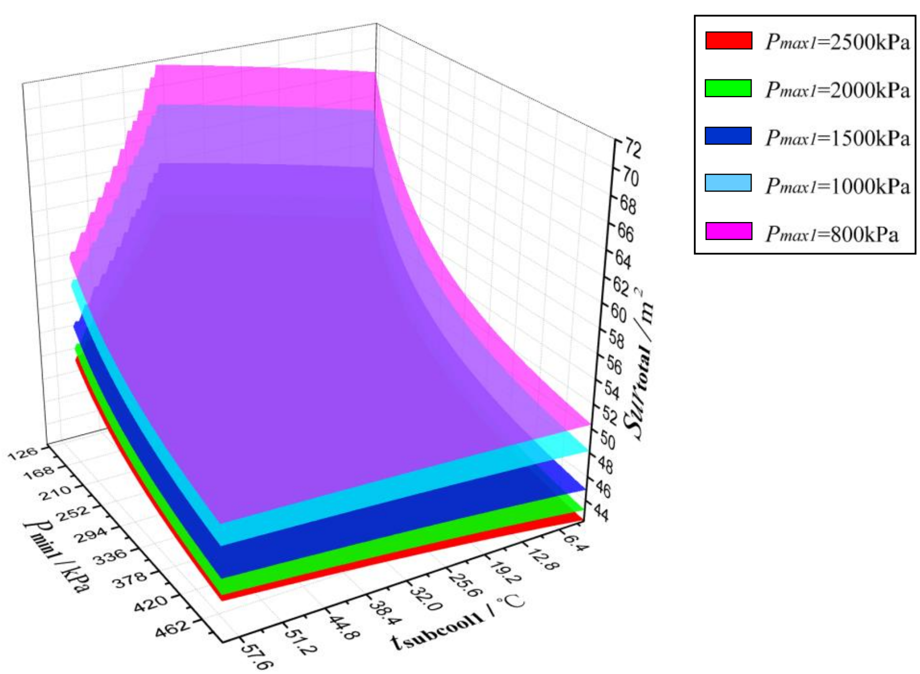

Fig. 13. Sur_{total} of DTORC under different P_{max1}.

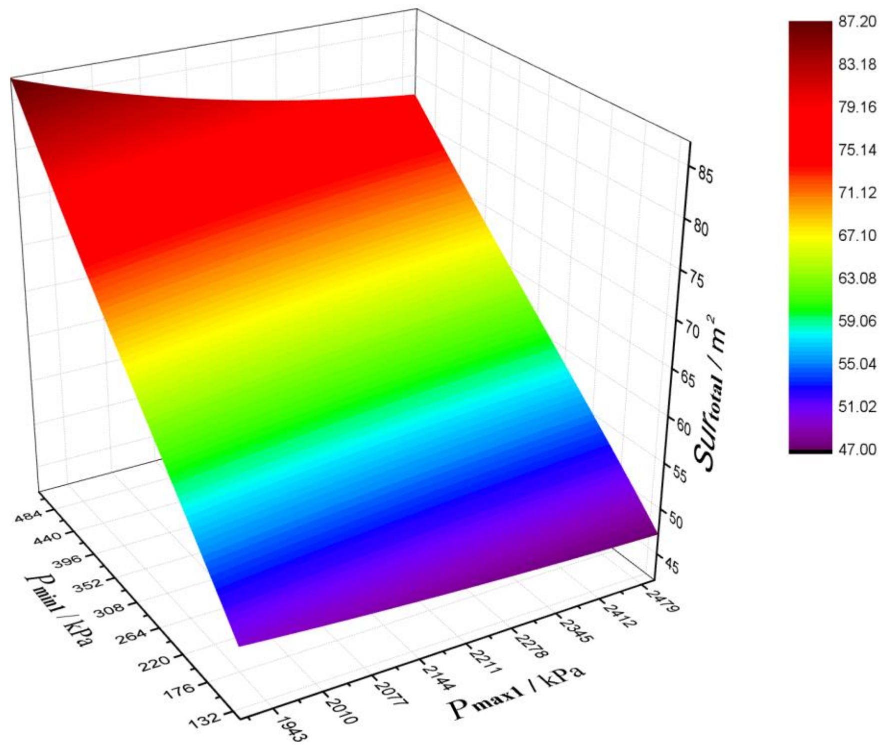

Fig. 14. Sur_{total} of RC with MM as the working fluid.

It is found that Sur_{total} and η_{net} are changed with an opposite trend both in RC and DTORC. For a fixed power output, the higher η_{net} is the lower Q_{ab} and Q_{dis} would be, which will lead to a reduction of Sur_{total}. It is also observed that when the optimal $\eta_{utilization}$ is reached, Sur_{total} is 47 m^2 in RC and 51 m^2 in DTORC. However, the minimum Sur_{total} of DTORC is 42 m^2 and that of RC is 47 m^2. The DTORC system has a higher $\eta_{utilization}$ *and* η_{net} than RC under the minimum Sur_{total} .

4.3. Respective power outputs of MM and R245fa in the DTORC

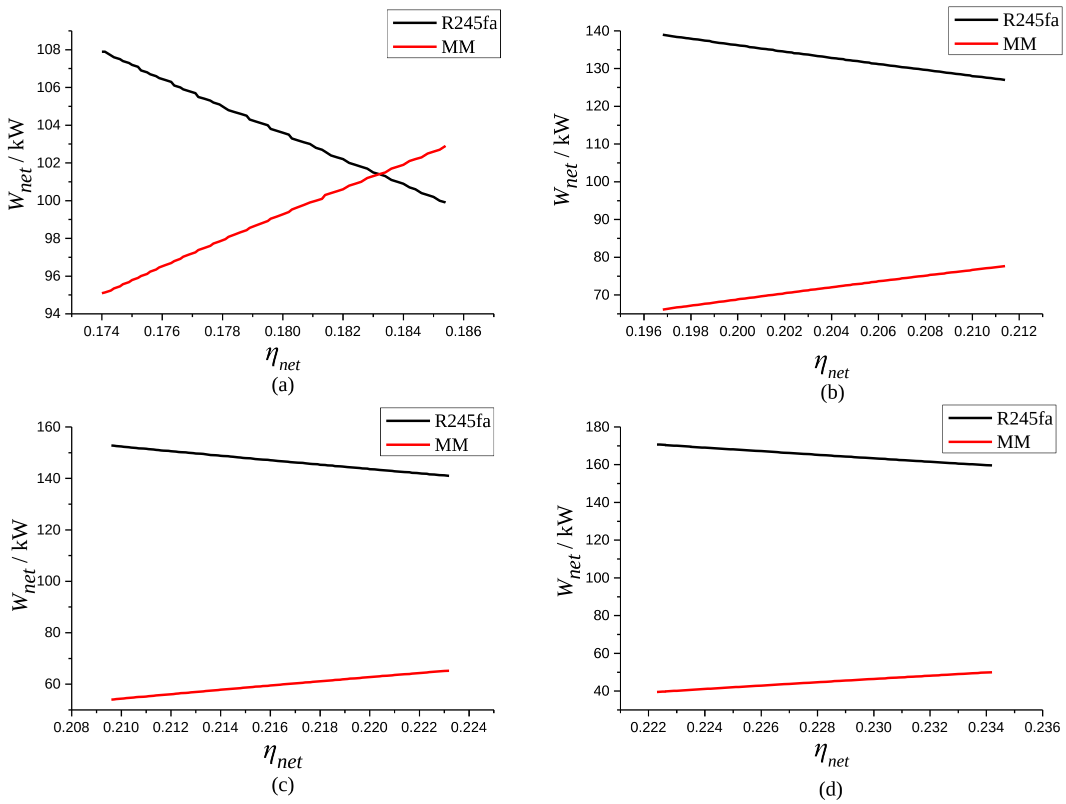

Fig. 15. Respective W_{net} of MM and R245fa in DTORC under $P_{max1} = 2000\text{kPa}$:(a) $P_{min1} = 120\text{kPa}$; (b)$P_{min1} = 216\text{kPa}$; (c)$P_{min1} = 308.1\text{kPa}$; (d)$P_{min1} = 500\text{kPa}$.

As shown in Fig. 15, it should be noted that $W_{net,MM}$ plus $W_{net,R245fa}$ equals 200 kW. In the DTORC system, R245fa obviously has a better work ability than MM. Therefore, with the increase of η_{net}, R245fa outputs more power and T_{max2} becomes higher and higher which may exceed the thermal decomposition temperature of R245fa. This should be avoided in the real applications. It should also be noted that with different combinations of organic fluids the trend of respective power outputs of the two stages may show different behaviors, due to the properties of the two working fluids. And the combination of the two working fluids could overcome the drawbacks of a single working medium.

5. Conclusions

A new deep super-cooling two-stage organic Rankine cycle (DTORC) is introduced to enhance both the thermal efficiency and heat source utilization at high temperature waste heat recovery. The performance of a DTORC system using MM and R245fa as the working fluids at high and low temperature stage is investigated in details. For the purpose of comparison, a RC system which uses MM as the working fluid under the same heat source at temperature of 300 °C is also studied. The optimal net thermal efficiency of DTORC can be up to 23.5%, whereas it can be up to 18% for RC. The optimal heat source utilization of DTORC is 16.3% whereas RC is 6.5%. The minimum Sur_{total} is 42 m^2 in DTORC and 47 m^2 in RC. Comparative analysis between DTORC and RC may lead to the following main conclusions:

•A new evaluation index, effective heat source utilization, is defined and it takes the whole heat source into account, which represents the working capacity of a thermal power system. High heat source utilization could have high power output under the same waste heat source.

•The DTORC system has higher heat source utilization, approximately 2.5 times of RC. The use of DTORC can increase the power output by 150% under the same mass flow rate of WHC.

•The maximum net thermal efficiency of DTORC could be up to 23.5%, which is increased by 30.5% at high temperature waste heat recovery applications compared with that in RC.

•The total surface area of heat exchangers in DTORC and RC are nearly equal. The minimum Sur_{total} of DTORC system is reduced by 10.6% compared with that in RC system.

Appendix

In Fig. 6(a):

$$P_2 = P_{max1} = P_3 = P_4 + P_{loss} = P_5 + P_{loss}$$

$$P_6 = P_7 = P_8 + P_{loss} = P_1 + P_{loss} = P_{min1} + P_{loss}$$

$$P_{10} = P_{max2} = P_{11} = P_{12} + P_{loss} = P_{13} + P_{loss}$$

$$P_{14} = P_{15} = P_{16} + P_{loss} = P_9 + P_{loss} = P_{min1} + P_{loss}$$

$$T_{HTFin} = T_{20} = T_4 + t_{pinch}$$

$$T_{HTFout} = T_{21} = T_3 + t_{pinch} = T_2 + t_{pinch}$$

$$(h_{20} - h_{21})\dot{m}_{HTF} = (h_4 - h_3)\dot{m}_{MM}$$

$$\frac{(h_{2s} - h_1)}{(h_2 - h_1)} = \eta_p, h_1 = h_8, W_{p,MM} = (h_2 - h_1)\dot{m}_{MM}$$

$$\frac{(h_5 - h_6)}{(h_5 - h_{6s})} = \eta_{exp}, h_6 = h_7, W_{exp,MM} = (h_5 - h_6)\dot{m}_{MM}$$

$$\frac{(h_{10s} - h_9)}{(h_{10} - h_9)} = \eta_p, h_9 = h_{16}, W_{p,R245fa} = (h_{10} - h_9)\dot{m}_{R245fa}$$

$$\frac{(h_{13} - h_{14})}{(h_{13} - h_{14s})} = \eta_{exp}, h_{14} = h_{15}, W_{exp,R245fa} = (h_{13} - h_{14})\dot{m}_{R245fa}$$

$$(h_7 - h_8)\dot{m}_{MM} = (h_{12} - h_{11})\dot{m}_{R245fa}$$

$$(h_{20} - h_{21})\dot{m}_{HTF} = (h_4 - h_3)\dot{m}_{MM}$$

$$Q_{ab,MM} = (h_4 - h_3)\dot{m}_{MM}, Q_{ab,R245fa} = (h_{12} - h_{11})\dot{m}_{R245fa}$$

$$Q_{dis,R245fa} = (h_{15} - h_{16})\dot{m}_{R245fa}$$

$$T_8 = T_{11} + t_{pinch} = T_{10} + t_{pinch}$$

$$T_7 = T_{12} + t_{pinch} = T_{13} + t_{pinch}$$

$$T_{16} = T_9 = T_{sur} + t_{pinch} = T_{22} + t_{pinch}$$

$$W_{net,MM} = W_{exp,MM} - W_{p,MM}, W_{net,R245fa} = W_{exp,R245fa} - W_{p,R245fa}$$

$$W_{net,sys} = W_{net,MM} + W_{net,R245fa}$$

$$\eta_{net} = W_{net,sys}/Q_{ab,MM}$$

$$\eta_{utilization} = W_{net,sys}/((h_{20} - h_{HTF,T_{sur}}) * \dot{m}_{HTF})$$

$$Sur_{total} = (Q_{ab,MM} + Q_{ab,R245fa} + Q_{dis,R245fa})/(3500 * t_{pinch})$$

In Fig. 6(b):

$$P_2 = P_{max1} = P_3 = P_4 + P_{loss} = P_5 + P_{loss}$$

$$P_6 = P_7 = P_8 + P_{loss} = P_1 + P_{loss} = P_{min1} + P_{loss}$$

$$P_{10} = P_{max2} = P_{11} = P_{14} + P_{loss} = P_{15} + P_{loss}$$

$$P_{16} = P_{17} = P_{19} + P_{loss} = P_9 + P_{loss} = P_{min1} + P_{loss}$$

$$T_{HTFin} = T_{20} = T_4 + t_{pinch}$$

$$T_{HTFout} = T_{21} = T_3 + t_{pinch} = T_2 + t_{pinch}$$

$$\frac{(h_{2s} - h_1)}{(h_2 - h_1)} = \eta_p, h_1 = h_8, W_{p,MM} = (h_2 - h_1)\dot{m}_{MM}$$

$$\frac{(h_5 - h_6)}{(h_5 - h_{6s})} = \eta_{exp}, h_6 = h_7, W_{exp,MM} = (h_5 - h_6)\dot{m}_{MM}$$

$$\frac{(h_{10s} - h_9)}{(h_{10} - h_9)} = \eta_p, h_9 = h_{19}, W_{p,R245fa} = (h_{10} - h_9)\dot{m}_{R245fa}$$

$$\frac{(h_{15} - h_{16})}{(h_{15} - h_{16s})} = \eta_{exp}, h_{16} = h_{17}, W_{exp,R245fa} = (h_{15} - h_{16})\dot{m}_{R245fa}$$

$$h_{12} - h_{11} = h_{17} - h_{18}$$

$$T_{18} = T_{11} + t_{pinch}$$

$$T_{17} = T_{12} + t_{pinch}$$

$$T_{12} = T_{13}$$

$$(h_7 - h_8)\dot{m}_{MM} = (h_{14} - h_{13})\dot{m}_{R245fa}$$

$$(h_{20} - h_{21})\dot{m}_{HTF} = (h_4 - h_3)\dot{m}_{MM}$$

$$Q_{ab,MM} = (h_4 - h_3)\dot{m}_{MM}, Q_{ab,R245fa} = (h_{14} - h_{13})\dot{m}_{R245fa}$$

$$Q_{rec,R245fa} = (h_{17} - h_{18})\dot{m}_{R245fa}$$

$$Q_{dis,R245fa} = (h_{18} - h_{19})\dot{m}_{R245fa}$$

$$T_8 = T_{13} + t_{pinch} = T_{12} + t_{pinch}$$

$$T_7 = T_{14} + t_{pinch} = T_{15} + t_{pinch}$$

$$T_{19} = T_9 = T_{sur} + t_{pinch} = T_{22} + t_{pinch}$$

$$W_{net,MM} = W_{exp,MM} - W_{p,MM}, W_{net,R245fa} = W_{exp,R245fa} - W_{p,R245fa}$$

$$W_{net,sys} = W_{net,MM} + W_{net,R245fa}$$

$$\eta_{net} = W_{net,sys}/Q_{ab,MM}$$

$$\eta_{utilization} = W_{net,sys}/((h_{20} - h_{HTF,T_{sur}}) * \dot{m}_{HTF})$$

$$Sur_{total} = (Q_{ab,MM} + Q_{ab,R245fa} + Q_{rec,R245fa} + Q_{dis,R245fa})/(3500 * t_{pinch})$$

References

[1] S. Lecompte, H. Huisseune, M. van den Broek, B. Vanslambrouck, M. De Paepe, Review of organic Rankine cycle (ORC) architectures for waste heat recovery, Renewable and Sustainable Energy Reviews, 47 (2015) 448-461.

[2] G. Xu, G. Song, X. Zhu, W. Gao, H. Li, Y. Quan, Performance evaluation of a direct vapor generation supercritical ORC system driven by linear Fresnel reflector solar concentrator, Applied Thermal Engineering, 80 (2015) 196-204.

[3] W.H.G.Y. Gao, Working fluid selection and preliminary design of a solar organic Rankine cycle system, Environmental Progress & Sustainable Energy, 34 (2015) 8.

[4] M.-H. Yang, R.-H. Yeh, Economic performances optimization of an organic Rankine cycle system with lower global warming potential working fluids in geothermal application, Renewable Energy, 85 (2016) 1201-1213.

[5] N. Kazemi, F. Samadi, Thermodynamic, economic and thermo-economic optimization of a new proposed organic Rankine cycle for energy production from geothermal resources, Energy Conversion and Management, 121 (2016) 391-401.

[6] M.-H. Yang, R.-H. Yeh, Thermodynamic and economic performances optimization of an organic Rankine cycle system utilizing exhaust gas of a large marine diesel engine, Applied Energy, 149 (2015) 1-12.

[7] J. Song, Y. Song, C.-w. Gu, Thermodynamic analysis and performance optimization of an Organic Rankine Cycle (ORC) waste heat recovery system for marine diesel engines, Energy, 82 (2015) 976-985.

[8] V. Zare, S.M.S. Mahmoudi, A thermodynamic comparison between organic Rankine and Kalina cycles for waste heat recovery from the Gas Turbine-Modular Helium Reactor, Energy, 79 (2015) 398-406.

[9] Y. Cao, Y. Gao, Y. Zheng, Y. Dai, Optimum design and thermodynamic analysis of a gas turbine and ORC combined cycle with recuperators, Energy Conversion and Management, 116 (2016) 32-41.

[10] B.N.-E. Peris, amp, Joaqu, amp, naMol, amp, F. s, amp, M.-B.A. lez, amp, c. na, Experimental characterization of an ORC (organic Rankine cycle) for power and CHP (combined heat and power) applications from low grade heat sources, Energy, 82 (2015) 8.

[11] L. Yingjian, Y.A. Abakr, Q. Qi, Y. Xinkui, Z. Jiping, Energy efficiency assessment of fixed asset investment projects – A case study of a Shenzhen combined-cycle power plant, Renewable and Sustainable Energy Reviews, 59 (2016) 1195-1208.

[12] B.N.-E. Peris, amp, Joaqu, amp, b. na, amp, F.-B.A. s, amp, c. na, Experimental study of an ORC (organic Rankine cycle) for low grade waste heat recovery in a ceramic industry, Energy, 85 (2015) 9.

[13] Q. Chen, G.P. Hammond, J.B. Norman, Energy efficiency potentials: Contrasting thermodynamic, technical and economic limits for organic Rankine cycles within UK industry, Applied Energy, 164 (2016) 984-990.

[14] J. Sarkar, Review and future trends of supercritical CO2 Rankine cycle for low-grade heat conversion, Renewable and Sustainable Energy Reviews, 48 (2015) 434-451.

[15] T. Erhart, J. Gölz, U. Eicker, M. van den Broek, Working Fluid Stability in Large-Scale Organic Rankine Cycle-Units Using Siloxanes—Long-Term Experiences and Fluid Recycling, Energies, 9 (2016) 422.

[16] B.G.Y.H. Dong, Analysis of zeotropic mixtures used in high-temperature Organic Rankine cycle, Energy Conversion and Management, 84 (2014) 8.

[17] M.a.E.b.M.M.a.C.A.c.A.c. Villarini, State of Art of Small Scale Solar Powered ORC Systems: A Review of the Different Typologies and Technology Perspectives, Energy Procedia, 45 (2014) 11.

[18] N.A. Lai, M. Wendland, J. Fischer, Working fluids for high-temperature organic Rankine cycles, Energy, 36 (2011) 199-211.

[19] D.W.C.H.b. Meinel, Effect and comparison of different working fluids on a two-stage organic rankine cycle (ORC) concept, Applied Thermal Engineering, 63 (2014) 8.

[20] G.M.D.P.G. Kosmadakis, Parametric theoretical study of a two-stage solar organic Rankine cycle for RO desalination, Renewable Energy, 35 (2010) 989-997.

[21] X. Xue, C. Guo, X. Du, L. Yang, Y. Yang, Thermodynamic analysis and optimization of a two-stage organic Rankine cycle for liquefied natural gas cryogenic exergy recovery, Energy, 83 (2015) 778-787.

[22] D.M. Thierry, A. Flores-Tlacuahuac, I.E. Grossmann, Simultaneous optimal design of multi-stage organic Rankine cycles and working fluid mixtures for low-temperature heat sources, Computers & Chemical Engineering, 89 (2016) 106-126.

[23] S. Safarian, F. Aramoun, Energy and exergy assessments of modified Organic Rankine Cycles (ORCs), Energy Reports, 1 (2015) 1-7.

[24] M. Khaljani, R. Khoshbakhti Saray, K. Bahlouli, Comprehensive analysis of energy, exergy and exergo-economic of cogeneration of heat and power in a combined gas turbine and organic Rankine cycle, Energy Conversion and Management, 97 (2015) 154-165.

[25] H.Y. Lee, S.H. Park, K.H. Kim, Comparative analysis of thermodynamic performance and optimization of organic flash cycle (OFC) and organic Rankine cycle (ORC), Applied Thermal Engineering, 100 (2016) 680-690.

[26] A. Hassoun, I. Dincer, Analysis and performance assessment of a multigenerational system powered by Organic Rankine Cycle for a net zero energy house, Applied Thermal Engineering, 76 (2015) 25-36.

[27] L. Li, Y.T. Ge, X. Luo, S.A. Tassou, Thermodynamic analysis and comparison between CO2 transcritical power cycles and R245fa organic Rankine cycles for low grade heat to power energy conversion, Applied Thermal Engineering, 106 (2016) 1290-1299.

[28] T. Li, J. Zhu, K. Hu, Z. Kang, W. Zhang, Implementation of PDORC (parallel double-evaporator organic Rankine cycle) to enhance power output in oilfield, Energy, 68 (2014) 680-687.

[29] N. Chagnon-Lessard, F. Mathieu-Potvin, L. Gosselin, Geothermal power plants with maximized specific power output: Optimal working fluid and operating conditions of subcritical and transcritical Organic Rankine Cycles, Geothermics, 64 (2016) 111-124.

[30] D.-x. Li, S.-s. Zhang, G.-h. Wang, Selection of organic Rankine cycle working fluids in the low-temperature waste heat utilization, Journal of Hydrodynamics, Ser. B, 27 (2015) 458-464.